Kinetic Study of Polyvinyl chloride (PVC) Pyrolysis with Characterization of Dehydrochlorinated PVC

Jiayang Wu,[1] Konstantinos G. Papanikolaou,[1] Feng Cheng,[1] Bennett Addison,[2] Amy A. Cuthbertson,[2] Manos Mavrikakis,[1] George W. Huber*

[1]Department of Chemical and Biological Engineering, University of Wisconsin, 1415 Engineering Drive, Madison, Wisconsin 53706, United States
[2]Renewable Resources and Enabling Sciences Center, National Renewable Energy Laboratory, 15013 Denver W Pkwy, Golden, CO 80401, United States

Abstract

In this paper we study the kinetics of polyvinyl chloride (PVC) decomposition using a combination of experimental and computational approaches. We develop a simplified kinetic model that contains only two steps: dehydrochlorination of PVC and further decomposition of PVC residue. The model is consistent with density function theory (DFT) calculations and experimental data. Dehydrochlorination is an autocatalytic reaction that starts with a tertiary chloride (Cl) and generates hydrogen chloride (HCl) and benzene as the main products. Benzene and HCl formation rates showed similar trends indicating that HCl likely catalyzes a homolytic carbon-carbon (C–C) bond cleavage, which gives rise to benzene and an aliphatic fragment. We characterized the structure of dehydrochlorinated PVC (PVC residue) using thermal gravimetric analysis (TGA), Fourier-transform infrared spectroscopy (FTIR), and nuclear magnetic resonance spectroscopy (NMR). FTIR and NMR results indicate that PVC residue contains 20% quaternary carbon content, indicating a high concentration of crosslinked molecules. We predict that the most probable structure in the crosslinked centers of PVC residue is cyclohexadiene, which is supported by DFT calculations, FTIR and NMR.

Key words: Plastic pyrolysis, PVC dehydrochlorination, Kinetic model, DFT calculations

1. Introduction

Polyvinyl chloride (PVC) is the third most widely used synthetic polymer after polyethylene (PE) and polypropylene (PP) in the United States and the fourth most used plastic in the world after PE, PP, and polyethylene terephthalate (PET).[1] As of 2020, global demand for PVC reached 43.4 million metric tons, with a 4.6% projected growth rate through 2025.[2] PVC and Polyvinylidene Chloride (PVDC) are commonly used as oxygen barriers in multilayer packaging materials.[3, 4] PVC and PVDC are also used in several other commonly used materials including: 1) credit cards, 3) PVC safety seals, 4) PVC liners, 5) PVC labels on PET bottles and 6) occasionally in rigid PVC bottles.[3, 5, 6] While PVC bottles constitute only a small percent of all rigids, globally over 576 ktons of PVC bottles were produced in 2020.[2] PVC is thus a common contaminant in waste plastics that can cause major concerns. For example in PET recycling as little as 100 ppm of PVC contamination can cause degradation and discoloration of PET.[7]

PVC is also problematic in thermal depolymerization or pyrolysis of waste plastics. Pyrolysis is a thermal method to convert waste plastics into plastic pyrolysis oils, which can be further upgraded by approaches such as steam reforming.[8-10] Over ten companies have made announcements that they are building or have built commercial plants to thermally degrade waste plastics into a pyrolysis oil.[11] The oil will be sent to steam crackers for further upgrading.[12] The chlorine concentration in the pyrolysis oil is directly associated with PVC removal efficiency at the waste sorting facility or potential dehydrochlorination processes during the thermochemical recycling method.[12, 13] If the Cl in PVC is not efficiently removed from the plastic mixture before pyrolysis, it causes corrosion on stainless steel pyrolysis reactors and steam crackers due to the formation of HCl.[14, 15] If the halogen forms organic halogen in the pyrolysis products, hydrotreatment is a prospective method to remove it, but has a significant cost.[16]

Pyrolysis of even a small amount of PVC can cause corrosion issues. For example, 1-3 wt% of PVC in the plastic waste feedstock leads to 5,000-10,000 ppm of chlorinated compounds in the final pyrolysis product.[17] In 1983, a German company added limestone ($CaCO_3$) to crushed waste plastic and processed the mixture in a rotary kiln reactor, pyrolyzed the waste plastics under temperatures from 400 ~ 500 °C.[14, 18] However, the chlorine content in the pyrolysis oil was above the requirements.[14] A Japanese company developed a dechlorination pre-treatment preceding the thermal degradation of mixed waste plastics. The plastic was mixed with calcium hydroxide ($Ca(OH)_2$) and introduced into a twin-screw unit operating at a temperature of 300 °C or higher, resulting in the removal of approximately 95% of chlorine through this process.[13, 14] However, the threshold of the chlorine content in modern industry facilities is 3 ppm.[12, 19] In addition, common stainless steel (304 and 316) are considered non-resistant to HCl at any concentration and temperature.[20] Thus, efficient removal of chlorine from mixed plastics wastes before pyrolysis is a critical technology.

PVC thermal decomposition occurs in two stages. In the first stage, approximately 65% weight loss occurs in a temperature range between 250 and 350 °C in an autocatalytic dehydrochlorination process that begins at structural defects like internal C=C bonds and butyl branches associated with tertiary Cl.[21, 22] In this stage, most of the Cl atoms are removed to form HCl molecules, with the remaining polymer forming π–conjugated polyenes.[23-28] After sufficient removal of Cl, the polyenes are unstable and thereby prone to form crosslinked intermediates as char precursors through pericyclic reactions.[15, 29] The main products of polyene degradation are multicyclic aromatic hydrocarbons, non-condensable gases, and chars.[30, 31]

There is ongoing debate about the mechanism of PVC thermal degradation. PVC decomposition can be described by either consecutive reactions[24, 31-35] or by competitive reactions.[36-38] In 1995, Beltran *et al.*[32] proposed a PVC degradation model involving two steps and three reactions: in the first dehydrochlorination stage, HCl and volatile compounds were generated through parallel reactions so that the first stage could be described as a parallel reaction model. In the second degradation stage, a model based on a single reaction corresponds to the pyrolysis of the polyene chains. In 2001, Jordan *et al.*[24] proposed a four consecutive step reaction model that involves: 1) PVC dehydrochlorination; 2) random chain scission reactions of dechlorinated PVC, 3) cyclization/aromatization, and 4) degradation from coke formation. In 2013, Gui *et al.*[34] suggested another PVC degradation mechanism involving four different stages: 1) dechlorination with inner cyclization, 2) scission of aromatic chains, 3) release of quasi-three rings or three rings, and 4) release of the two-ring group. In 2020, Xu *et al.*[33] proposed a more complex PVC dehydrochlorination model that involved four consecutive reactions and fit this model to TGA data.

Previous models seldom predict Cl removal efficiency in dehydrochlorination process, and the degradation stages for dechlorinated PVC were difficult to define. For example, in the Jordan *et al.* model,[24] the cyclization rate would be difficult to determine if some polyaromatics remained on the PVC carbon back chain. In the Gui *et al.* mechanism,[34] the third and fourth stage could be difficult to distinguish in order to calculate the kinetics for each stage.

In this study, we developed a simpler model that contains two steps: dehydrochlorination of PVC and further decomposition of PVC residue. A first order reaction model of dehydrochlorination PVC was used to predict the Cl removal efficiency, and a lumped model was used to predict the overall mass loss of further decomposition of PVC residue. The model in the dehydrochlorination stage was consistent with DFT calculations and can predict the residual Cl content during the pretreatment till 0.1 wt. %. In addition, we characterized the structure of PVC residue using TGA, FTIR, and NMR. These results provide insight into the final structure of PVC residue, which may be used for further upgrading through pyrolysis or mechanical recycling.

2. Experimental methods

2.1 Materials

Plastics: PVC (#81387) was obtained from Sigma-Aldrich, and both Polystyrene (PS 608A) and Low-density polyethylene (LDPE 524B) were obtained from Amcor. The PVC was used without modification. PS and LDPE were mixed by cryogrinding with a 1:1 ratio to prepare the standards on NMR analysis.

Gas chromatography (GC) standards: Benzene (#401765) and the polyaromatic hydrocarbon standards (EPA 8270 Calibration Mix 1, #5M00720) were obtained from Sigma-Aldrich.

2.2 Thermogravimetric analysis (TGA) of PVC

TGA was carried out using a TA Instruments SDT Q500 system with nitrogen (N_2) used as the sweep gas. Different N_2 flow rates (50-200 sccm) and sample weights (2-10 mg) were used in the experiments. The PVC particle sizes are less than 80 mesh (174 micron) with a molecular weight of 90,000 Da. To study the PVC dehydrochlorination process, 10 mg PVC was heated to 320 °C with a temperature ramping rate of 2 °C/min and held at 320 °C isothermally for 20 min. To obtain the data for our kinetic model, 10 mg PVC was heated to 600 °C with a temperature ramping rate of 10 °C/min.

2.3 PVC pretreatment system

The pretreatment system setup is shown in Figure 1. The system contained two sets of gas treatments for (1) collecting the organic product and (2) removing the generated HCl. Nitrogen was used as the inert gas with a flow rate at 100 sccm. The temperature of the reactor was ramped from room temperature to 320 °C with a 2 °C/min ramping rate and held isothermally for 20 min. For each batch, 1-10 g of PVC was used.

For collecting the organic effluents released from the dehydrochlorination process, the system was connected to a dodecane trap, which was composed of three bubblers with 10 mL dodecane in series. The dodecane solution collected in each condenser was analyzed using a GC shown in section 2.41. Excess Na_2CO_3 powder was mixed with the PVC in the reactor to capture the generated HCl.

For collecting the dehydrochlorinated PVC, no base was mixed with PVC in the reactor, so the system was connected to three adsorbers in series to remove the generated HCl. The adsorbers were filled with a mixture of calcium hydroxide powder and alumina pellets. The dehydrochlorinated PVC obtained from the pretreatment system will be referred to as PVC residue later in the paper.

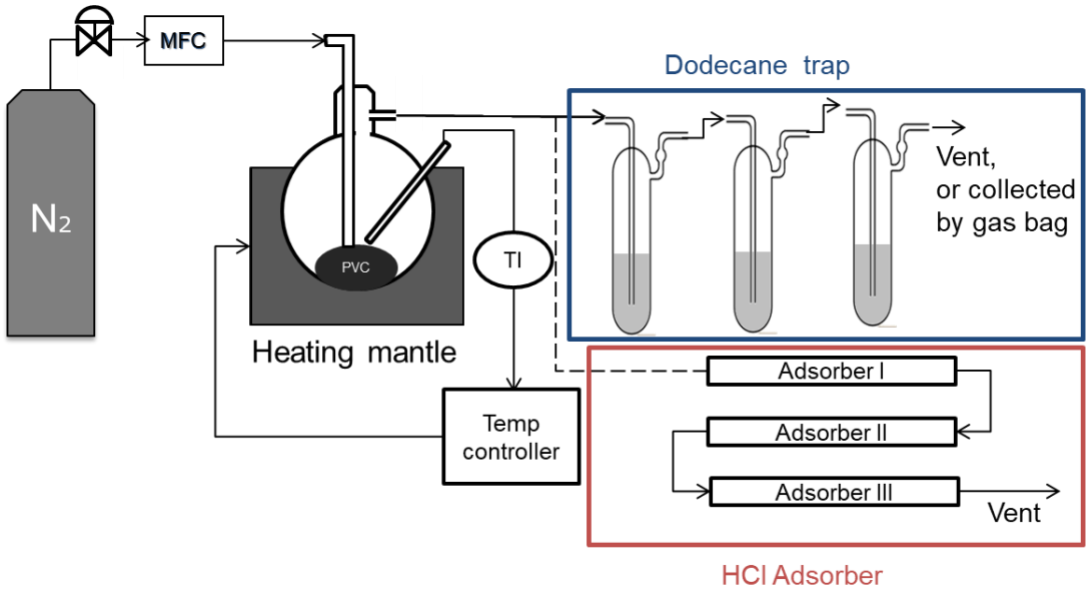

Figure 1. Reactor scheme of PVC thermal pretreatment system.

2.4 Characterization of PVC residue

2.4.1 GC- Flame ionization detection (GC-FID)

The liquid products collected from the dodecane trap were analyzed by GC- FID using Shimadzu GC-2010 with an RTX-VMS column. The temperature of the GC was held at 40 °C for five minutes and

then increased to 240 °C with a ramping rate of 7.5 °C/min and held for 10 minutes. The temperature of the FID detector was 240 °C. Products were quantified using external standards.

2.4.2 TGA

Ten mg of PVC residue was tested using a TGA with a TA Instruments SDT Q500 system (same as the above). The sample was heated to 600 °C with the purge of nitrogen 50 sccm at a temperature ramp rate of 10 °C/min.

2.4.3 FT-IR spectroscopy

A Bruker Vertex 70 with a liquid nitrogen-cooled MCT detector was used for the FTIR-ATR analysis. A MIRacle single reflection cell with a diamond crystal was utilized as the ATR cell (Pike Technologies). The samples were tested with 128 scans, a resolution of 4 cm^{-1}, and a range of 4000-600 cm^{-1}.

2.4.4 GC-MS/FID Polyarc analysis of extractable compounds

Five hundred to seven hundred mg of the PVC residue was extracted using 25 mL of dichloromethane in amber borosilicate hermetically sealed vials. Vials were sonicated for 10 minutes prior to equilibrating in the dichloromethane for 10 days. Polyaromatic hydrocarbons have low solubility and high affinity for solids, and therefore equilibration times are long (at least 7 days in water depending on the molecular weight).[39] The extract was filtered and the remaining PVC residue was rinsed with 5 mL of dichloromethane, for a total of 30 mL extract. The dichloromethane extract was concentrated to 1 mL under a gentle stream of nitrogen and then spiked with 5 µL internal standard (EPA 8270 deuterated internal standard mix from Sigma Aldrich). Quantification of PAHs and estimation of unknowns were analyzed using an Agilent GC- mass spectroscopy (MS)/FID Polyarc. Details on analysis including standard information, GC-MS conditions, and chromatograms are included in electronic supplementary materials (ESI) Text S1 and Figure S1. The cleaned PVC residue was dried for 24 hours at 40 °C, and then analyzed by NMR.

2.4.5 Solid-state NMR

All solid-state NMR experiments were collected using a 600 MHz Bruker Avance-III NMR spectrometer equipped with a PhoenixNMR HXY MAS probe with a 4 mm probe head, configured in HX dual resonance mode. Approximately 50 mg of each material was center-packed into thin-walled 4 mm Revolution NMR zirconium rotors and sealing spacers. All data was collected using 14 kHz MAS. For all experiments, typical hard pulses were 4 µs for ^{13}C and either 3.15 or 4.0 µs for ^{1}H, cross-polarization (CP) was achieved a square 60 kHz RF spin-lock pulse on the ^{13}C channel, and a 10% linear ramped spin-lock pulse on the ^{1}H channel set to the +1 sideband of the Hartman-Hahn profile. Near-quantitative ^{13}C spectra were obtained using the composite pulse MultiCP pulse sequence[40] using the following parameters: 7 ramped cross-polarization steps of 1100 µs each and a 1100 µs final CP step, a 0.8 second proton polarization delay, a 0.5 second recycle delay, and a rotor-synchronized Hahn-echo was used prior to acquisition for a clean baseline. 84 kHz ^{1}H decoupling (Bruker sequence swftppm) was used during both the Hahn echo and during acquisition. MultiCP conditions were optimized using cryomilled model aromatic-containing and aliphatic-containing polymers PS and LDPE.

2D ^{13}C-^{1}H Frequency-Switched Lee-Goldberg Heteronuclear Correlation (FSLG-HETCOR)[41] data were collected using the lghetfq Bruker pulse sequence. To observe correctly scaled ^{1}H chemical shifts, which evolve under the LG condition in the indirect dimension, we set from l0 to 3 and allowed for the pulse sequence to directly account for the scaling factor of 0.577. ^{1}H shifts were referenced externally to TMS at 0 ppm by acquiring the identical FSLG-HETCOR experiment on crystalline α-glycine, for which the observed ^{1}H shifts for the CH_2 site were set to 3.8 and 2.6 ppm.[42, 43] The experiment was collected using a short (100 us) cross-polarization time to preferentially observe directly bonded CH pairs. All data were processed using MestreNova version 14.

2.4.6 Total halogen analysis

The PVC residue samples were sent to Huffman Hazen Laboratories (Golden, CO) for a total halogen analysis. A Mitsubishi TOX-100 instrument was used with a dual zone high temperature (800 °C/900 °C) quartz combustion furnace in an oxygen atmosphere. This converted any halogen to halides and oxyhalides. These compounds then were transported to an absorber solution within a coulometric cell and titrated against silver to the potentiometric endpoint. Since pure PVC only contains Cl, all detected halogens were measured as Cl.

2.5 Computational details

The formation of benzene from polyene chains was modelled by means of DFT calculations using Gaussian 09.[44] All calculations were performed at the M06–2X/6–31++g (d,p) level of theory and the computed Gibbs free energies are reported at 327 °C.[45, 46] This level of theory is appropriate for computational studies of thermal decomposition of PVC.[15] All reported transition states had a single imaginary frequency that involved motion along the reaction coordinate, whereas there was no imaginary frequency for states that represent stationary points in the potential energy diagram (PED).

3. Results

3.1 Quantification of organic products generated from PVC dehydrochlorination

Figure 2 shows the TGA result for PVC decomposition. The red line represents the TGA temperature program and the black line represents the normalized weight loss of PVC. The PVC was 1) ramped at a rate of 2 °C/min from room temperature to 320°C, 2) held at 320 °C for 20 min, and 3) heated to 600°C with a ramp rate of 2 °C/min. The dash lines show the mass loss for the first two stages of the TGA temperature program (the PVC dehydrochlorination process). In the first stage, 53.1 wt.% of the original mass of PVC was lost, and in the second stage, 8.3 wt.% of the PVC was lost. The first stage mass loss is due to the release of Cl from PVC where the solid PVC forms an unstable polyene species.[25] The polyene then starts cyclization and decomposing into aromatics, non-condensable gases, and polyaromatics/coke species during the second stage.[25, 30]

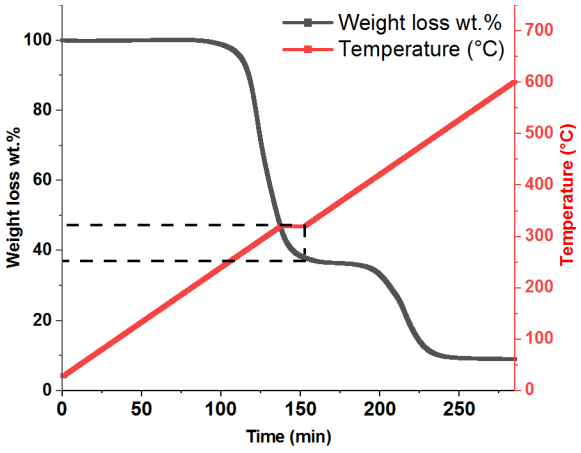

Figure 2. PVC degradation in TGA with a ramping rate of 2 °C/min from room temperature to 320 °C, held at 320 °C for 20 min, then ramped 2 °C/min to 600°C, with a 50 sccm N_2 flow.

In the PVC pretreatment system, 1g of PVC was mixed with 3g of Na_2CO_3 and decomposed at the same temperature program shown in Figure 2. This allowed us to quantify the aromatic formation during the pretreatment process. The aromatics were condensed in a dodecane solution and analyzed by GC-FID. Benzene was the only detected chemical in the dodecane trap by GC-FID and accounted for 2.8 wt.% of the initial PVC mass. This is consistent with other literature studies where HCl and benzene are coproduced.

[30, 33] The amount of HCl formed was estimated from the stoichiometric composition of pure PVC, which is 58.4 wt.%. The overall mass loss obtained from the pretreatment system was 61.2 wt.%, which is consistent with the TGA result (61.4 wt.%). Therefore, both PVC pretreatment and TGA results suggest that the main volatile products of PVC dehydrochlorination are HCl and benzene.

A previous study reported that both naphthalene and anthracene are trace products from the dehydrochlorination of PVC,[33] and DFT calculations have shown that Gibbs free energy barriers associated with the formation of such products are substantial (> 200 kJ/mol).[47] We did not see these products using GC-FID. We used dichloromethane to extract any compounds in the PVC residue and analyzed by GC-MS. Traces of the polyaromatic hydrocarbons, such as naphthalene, methylnaphthalene, anthracene, and phenanthrene were detected, as well as many unknown species. Detailed extraction results are shown in Figure S1 and Table S1 in the ESI. Grimes *et al*. and Gui *et al*. also reported that heavier aromatics were generated after the PVC dehydrochlorination stage.[34, 48] We estimated the yields of these polyaromatic hydrocarbons to be less than 0.08 wt. %.

3.2 Stepwise benzene formation and quantification during PVC dehydrochlorination

Aromatic compounds are mainly generated in the second stage (the degradation of polyenes) of PVC degradation with small amounts of benzene forming during the first stage.[30] A stepwise benzene quantification could help estimate the benzene formation rate and better understand the chemistry of PVC dehydrochlorination.

Gas products generated from the PVC dehydrochlorination were collected in a dodecane trap connected with a gas bag in the PVC pretreatment system. Temperature segments of 20 °C from 140 to 320 °C were used for these experiments. The collected sample in the dodecane traps and the gas bags were quantified by GC-FID. Benzene was the only product detected by the GC. The benzene formation rate was calculated by the mass detected by the GC divided by the time collected for each trap. Figure 3 shows that the DTG of PVC's TGA curve and the benzene generation rate follow similar trends with temperature. Benzene formation starts at 220 ~ 240°C. The quantity of benzene generated (2.8 wt.%) during dehydrochlorination was observed to be notably lower than the stoichiometry generation of HCl (58.4 wt.%). Therefore, the derivative thermogravimetric (DTG) curve was employed to depict the rate of HCl formation, suggesting the formation rates of both benzene and HCl follow a similar trend. HCl could potentially catalyze benzene formation during the dehydrochlorination process. This hypothesis is further examined in section 3.3, where the DFT results are presented.

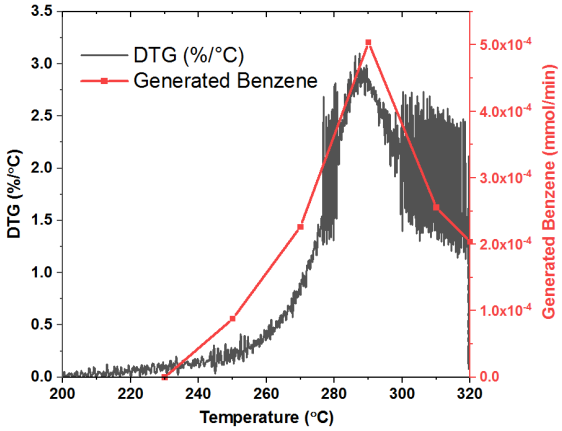

Figure 3. Comparison of the first derivative of TGA (PVC dehydrochlorination signal) and the rate of benzene formation with a temperature ramp rate of 2 °C/min.

3.3. DFT calculations of benzene formation during PVC dehydrochlorination

The detailed benzene formation mechanism predicted by our DFT calculations is shown in Figure 4. DFT calculations support the synergistic effect between dehydrochlorination and benzene formation demonstrated by TGA in Figure 3. Figure 4a shows the Gibbs free energy diagram for benzene formation starting from a single polyene chain via a conventional pathway reported in the literature.[15] This pathway is intramolecular and involves the cyclization of a polyene chain to cyclohexadiene followed by a bond cleavage.[49] It begins with three isomerization reactions of the polyene (**S1** → **S2**, **S2** → **S3**, **S3** → **S4**) before a ring closure reaction (**S4** → **S5**) (Figure 4c and Figure S2 in the ESI), which gives rise to a cyclohexadiene ring (**S5**) (Figure 4c and Figure S2 in the ESI). The latter reaction step is exergonic by 56.0 kJ/mol and requires a Gibbs free energy barrier of 131.0 kJ/mol (Figure 4a). The isomerization reactions exhibit low Gibbs free energy barriers except for **S2** → **S3.** This step involves a rotation around a double bond and has a high activation energy barrier (287.0 kJ/mol) (Figure 4a). After ring closure, the formation of benzene occurs via an atomic hydrogen abstraction from **S5** followed by a homolytic C–C cleavage (**S6** → **S7** Figure 4a and Figure S2 in the ESI). The short segment shown in **S6** and **S7** in Figure 4c refers to the residual polyene chain after the benzene cleavage. We compute that the effective Gibbs free energy barrier from **S5** to **S7** is 345.0 kJ/mol (Figure 4a).

We found that the C–C cleavage reaction step (**S6** → **S7** in Figure 4a and Figure 4c), which is kinetically the least favorable in the conventional pathway (Figure 4a), may be catalyzed by HCl (Figure 4c and Figure S2 in the ESI). HCl catalysis is likely to occur during the dehydrochlorination stage where a considerable amount of HCl is released from PVC. This is corroborated by the presented experimental data in Figure 3. The HCl–catalyzed C–C cleavage takes place via a hydrogen exchange, whereby HCl withdraws a hydrogen from the cyclohexadiene ring and donates its hydrogen to the aliphatic fragment. Structure S5 decomposes directly to ethylene and benzene in the presence of HCl (**S5** → **S6** via **TS5** in Figure 4b and Figure 4c). This concerted process requires a Gibbs free energy barrier of 276.0 kJ/mol, which is lower than that for the **S5** → **S7** reaction step in the conventional pathway (Figure 4a) by 69.0 kJ/mol. Therefore, the DFT results obtained here confirm that benzene formation is catalyzed by HCl, thereby justifying the detection of benzene in the first decomposition stage of PVC.

This result may help understand char formation at the final stage of pyrolysis. At the end of the 2nd stage of PVC degradation, there is little Cl in the system, and the energy barrier of benzene formation becomes high. Thus, the carbon backbones tend to build more crosslinks and form chars instead of forming aromatic compounds.

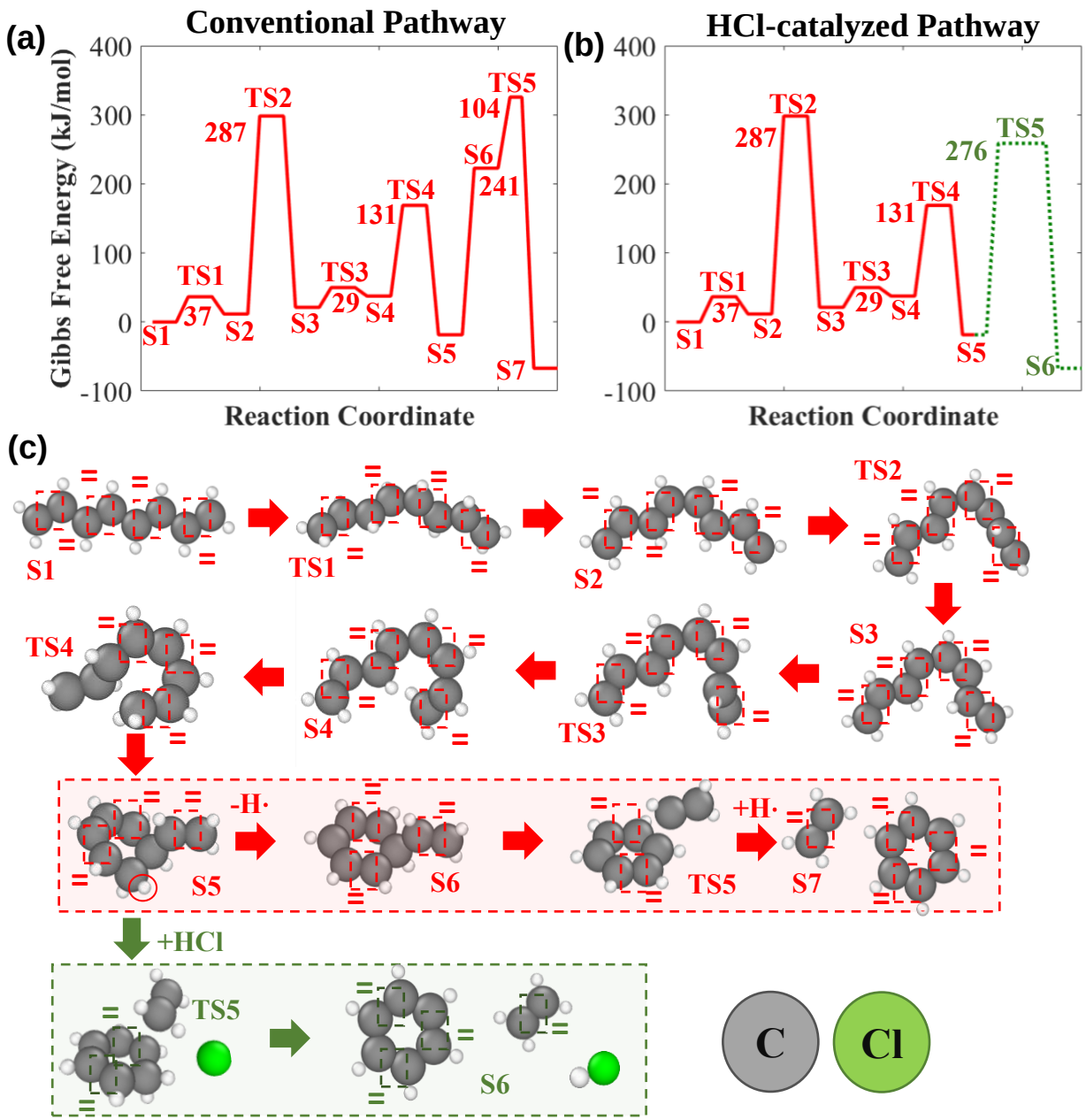

Figure 4. (a) Gibbs free energy diagram for the formation of benzene via a conventional pathway (red line). (b) Gibbs free energy diagram for the formation of benzene via a catalyzed pathway by HCl (green dashed line); the two pathways are alike up to state S5, but they differ in the way the C–C cleavage occurs (green dotted line in panel b). The numbers in the plot represent Gibbs free energy barriers in kJ/mol. (c) Optimized structures for the initial, final and transition states of the two pathways. States that are involved only in pathway 1 (pathway 2) are shaded in red (green). C, Cl and H atoms are shown with grey, green and white circles, respectively. Gibbs free energies are reported at 327 °C. Double bonds are indicated by an equal sign and a dashed square on the molecular structures. The hydrogen atom that is abstracted from the ring of S5 is marked with a red solid circle.

3.4 Kinetic model for PVC degradation

PVC degradation occurs in two mains steps: (1) dehydrochlorination followed by (2) the decomposition of the crosslinked intermediates.[28, 30, 32, 37, 38] During the PVC dehydrochlorination only 2.8 wt.% of the mass of the PVC converts to benzene. Therefore, to simplify the modeling process on PVC dehydrochlorination stage, we assume that the formation of benzene (second step) is negligible during the PVC degradation at temperatures lower than 320 °C. The PVC degradation model can be divided into two regions: (1) below 320 °C, where dehydrochlorination dominates, which is a first order reaction and (2) above 320 °C, where the decomposition of the crosslinked intermediates is the prevailing process, which is a random scission reaction that generates mainly aromatics and some non-condensable gases.[24]

The Arrhenius equation (Eq 1) was used to fit the PVC degradation data for both stages. In the first degradation stage, the Arrhenius equation was modified into Eq 2 to obtain the kinetic of dehydrochlorination. *A* represents the Arrhenius pre-exponential factor, *R* represents the gas constant, E_a represents the activation energy, *T* represents the temperature, and *ß* represents the heating rate. The x in Eq 2 and Eq 3 represent the normalized non-decomposed PVC (PVC residue). The *w* in Eq 3 represents the current weight, w_0 the initial weight, and w_f the weight of the char formed after the pyrolysis process.

$$k = Aexp(\frac{-Ea}{RT}) \quad \text{(Eq 1)}$$

$$k_{HCl} = \frac{\partial x}{dT} = \frac{A_{HCl}}{\beta}\exp\left(\frac{-Ea_{HCl}}{RT}\right)(1-x) \quad \text{(Eq 2)}$$

$$x = \frac{w}{w_0 - w_f} \quad \text{(Eq 3)}$$

In the second degradation stage, PVC residue forms a polyene-like structure, which is further thermally decomposed by random-scission reactions.[24] Zhao *et al*. reported a parallel first order random-scission reaction that can describe polyethylene degradation better than a single first order model.[50-52] We applied this model to simulate the polyene decomposition process. The single first order model (k_{CI_single}) is derived from Arrhenius equation directly shown as Eq 4 to describe the decomposition of the crosslinked intermediates. The parallel model for the crosslinked intermediates ($k_{CI\_parallel}$) is shown as Eq 5. The AIC statistical analysis Eq 6 was used to compare different proposed models.[52-54] The RSS represents the residual sum of squares, *n* represents the total data points (sample size), and *k* represents the number of estimated parameters in the model.

$$k_{CI\_single} = \frac{\partial x}{dT} = \left[\frac{A_1}{\beta}\exp\left(\frac{-Ea_1}{RT}\right)\right](1-x) \quad \text{(Eq 4)}$$

$$k_{CI\_parallel} = \frac{\partial x}{dT} = \left[\frac{A_1}{\beta}\exp\left(\frac{-Ea_1}{RT}\right) + \frac{A_2}{\beta}\exp\left(\frac{-Ea_2}{RT}\right)\right](1-x) \quad \text{(Eq 5)}$$

$$AIC = nln\left(\frac{RSS}{n}\right) + 2k \quad \text{(Eq 6)}$$

The final expression of the PVC decomposition is a linear combination of first and second decomposition stage, as shown in Eq 7. α represents the normalized mass loss of the PVC. m_{HCl} and m_{CM} are the mass of HCl and crosslinked intermediates, respectively. These two values are calculated from the mass loss of the 1st and 2nd stage of PVC degradation. Two PVC kinetic models are proposed here: the main difference between Model I and Model II is that Model I refers to the single first order decomposition of PVC residue ($k_{CI} = k_{CI\_single}$) and Model II refers to the parallel first order decomposition of PVC residue ($k_{CI} = k_{CI\_parallel}$).

$$\alpha = m_{HCl}[-1 \times \exp(-k_{HCl} \times t) + 1] + m_{CI}[-1 \times \exp(k_{CI} \times t) + 1] \quad \text{(Eq 7)}$$

The "nlinfit" function in Matlab was used to fit the model (*A* and E_a) parameters to the experimental data by minimizing the residual sum of squares (RSS). Figure 5a and 5b compare the actual TGA mass loss to Models I and II. Figure 5c and 5d show the zoomed in spectrum of the secondary PVC degradation stage. The fitted parameters for PVC degradation are shown in Table 1 with a 95% confidence interval. Model II better describes the second stage of PVC decomposition according to the AIC equation as shown in Table 2 and Figure 5. The kinetic model for PVC degradation that best fits the data thus contains two stages: a

first order reaction model for the dehydrochlorination, and a parallel first order reaction model for the further thermal decomposition of polyenes.

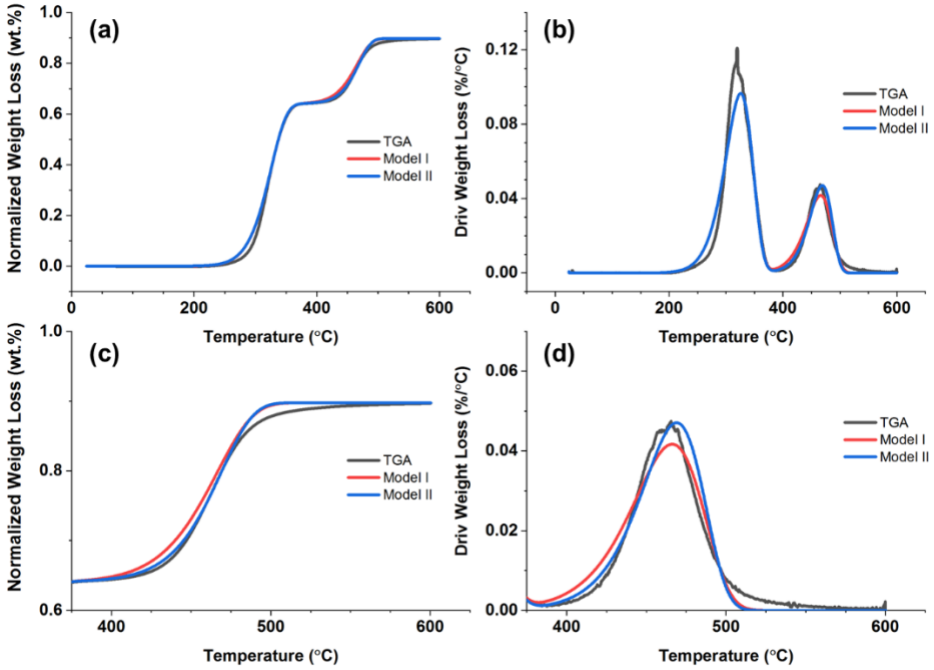

Figure 5. Comparison of weight loss curve of PVC between model and experimental results, including (a) TGA, (b) DTG with 10 °C/min ramping rate to 600 °C with both first stage degradation, (c) zoomed in secondary degradation of TGA, and (d) DTG results.

Table 1. Kinetic parameters for PVC degradation. Rate constants (*k*) correspond to reactions shown in Figure 5.

	PVC Model I			PVC Model II	
	E_a (kJ/mol)	A (s^{-1})		E_a (kJ/mol)	A (s^{-1})
k_1	115.72 ± 0.69	$8.63\times10^{6} \pm 1.23\times10^{5}$	k_1	115.72 ± 0.69	$8.63\times10^{6} \pm 1.23\times10^{5}$
k_3	201.24± 1.32	$3.05\times10^{12} \pm 4.84\times10^{9}$	k_3'	5.98 ± 0.03	$3.6\times10^{-3} \pm 2.08\times10^{-5}$
			k_3''	230.60 ± 1.24	$5.8\times10^{12} \pm 3.2\times10^{9}$

Table 2. AIC values for PVC models

Model	Number of parameters	RSS	Sample size N	AIC_C
PVC model I	4	0.56	3757	-3.31×10^{4}
PVC model II	6	0.48	3757	-3.37×10^{4}

The kinetic model was further validated by both TGA isothermal experiments and DFT calculations. Ten mg of PVC was tested on PVC at 210 and 300 °C isothermally for 2 h. The kinetic model accurately predicted Cl loss for these isothermal experiments (Figure S3 in the ESI). DFT calculations verified the catalytic effect of HCl in the dehydrochlorination reaction step. Figure S4 in the ESI shows the DFT–computed initial, transition and final state structures for the HCl–catalyzed and non-catalyzed dehydrochlorination. The DFT calculated dehydrochlorination energy barrier with HCl autocatalysis is 135 kJ/mol which is in reasonable agreement with the experimental barrier of 116 kJ/mol.[47] Also, we have

previously shown that dehydrochlorination barriers of 110 kJ/mol are observed at increasing π-conjugation lengths.[47]

3.5 Quantification of the residual Cl content

Four PVC residue samples were characterized by total halogen analysis using the followed temperature program: increases to 320 °C with a ramping rate of 2 °C/min and hold isothermal for 20 min. The Cl removal degree was calculated by Eq 8. The initial theoretical Cl was obtained from stoichiometry. The average Cl removal degree for the four pretreatment samples was 99.69% with a standard deviation of 2.944×10^{-4}. These results confirm that a lower temperature treatment can remove the majority of Cl from PVC. The remaining Cl may form some organic chlorine compounds during the PVC second degradation step.

$$\text{Cl removal degree} = \left(1 - \frac{\text{Cl content in the PVC residue}}{\text{Initial theoretical Cl content in virgin PVC}}\right) \times 100\% \quad \text{(Eq 8)}$$

To further improve the Cl removal efficiency, we extended the isothermal treatment at 320 °C from 20 min to 40, 60, and 480 min. The Cl content decreased with increasing treatment time. Our kinetic model (k_1) can be used to accurately predict the amount of residual Cl when the Cl content was above 0.1 wt.%, as shown in Figure 6a.

3.6 FT-IR spectroscopy of PVC residue

FT-IR spectroscopy was used to characterize the PVC residue, virgin PVC, and virgin PE. The PVC residue is the residue prepared by PVC thermal treatment shown as Figure 1. The assignments of the peaks are shown in Table 3 and Figure 6b. There are two major differences between the spectra of PVC residue and virgin PVC. First, in the spectrum of virgin PVC, the highest peak is shown in 608 cm^{-1}, which corresponds to the C-Cl peak.[55] This peak decreases in the PVC residue spectrum, indicating most of Cl was removed from the PVC. This statement is supported by both TGA (Figure S5 in the supplementary information) and total halogen analysis. Second, there are two peaks at 1600 cm^{-1} and 3020 cm^{-1} in the spectrum of the PVC residue, while the same peaks are not observed in the spectrum of virgin PVC; these peaks have assigned to aromatic structures in the literature.[56, 57] However, since aromatics exhibit a conjugated-π system,[58] these two peaks could also represent the conjugated π-bond structures, contributing via the crosslinked polyene structures.[47]

Both virgin PVC and the PVC residue have a peak at around 1440 cm^{-1}, which represents the methylene group (alkene structure).[56, 59] For the virgin PVC, internal double bond defects could cause this peak, while for the PVC residue, the double bond structures could be the remaining double bonds after crosslinking between polyenes. Therefore, the FT-IR results confirm the majority of Cl is removed during dehydrochlorination of PVC, and that the residual PVC backbone is likely composed of a crosslinked center with conjugated π-bonds, and surrounding structures with PE-like alkyl structure with some double bonds.

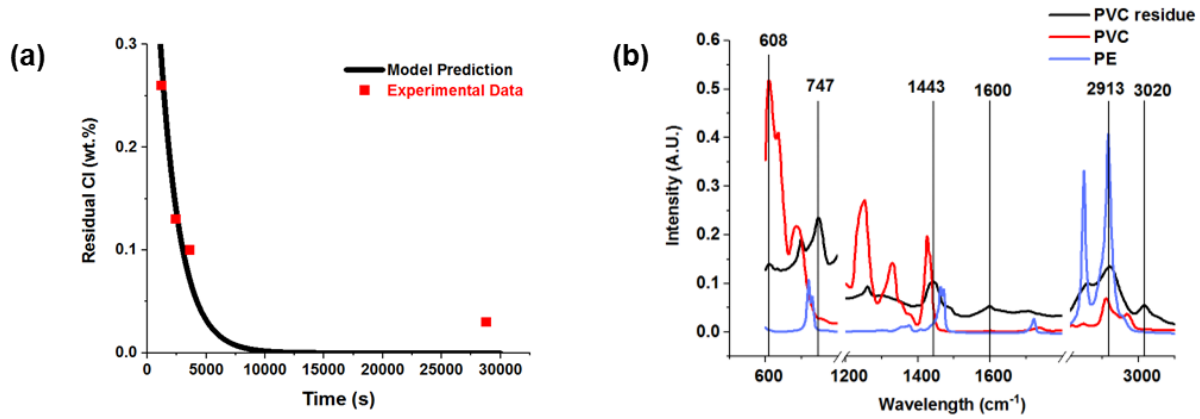

Figure 6. (a) PVC first stage degradation model (k1) prediction of Cl removal with the experimental data. (b) FT-IR spectra of PVC residue, pristine PVC, and PE

Table 3. Assignments of FT-IR peaks reported in the literature.

Bond type	**Adsorption Band (cm^{-1})**
C=C-H stretching (conjugated π system)	3000~3100[60]
Alkyl C–H stretching	2850-2920[61]
conjugated π C=C	1600[56], 740[56, 57]
Alkene C=C scissoring	1422-1453[57, 59]
C-Cl stretching	600-800[55]

3.7 ^{13}C Solid-state NMR analysis of PVC residue

The PVC residue was extracted and washed with dichloromethane before NMR analysis to remove extractable organics. Seventy-eight extractable compounds were identified, of which 11 were known polycyclic aromatic hydrocarbons and 67 were unknown structures. The semi-quantification total estimation of these extractable organics accounted for 0.07-0.08 wt.% of the PVC residue mass. A table including the total weight for each compound and sum total wt.% can be found in Table S1 in ESI. The ^{1}H-^{13}C multiple cross-polarization magic angle spinning (MultiCP-MAS) solid-state NMR method provides quantitative information related to carbon structures without the need for long relaxation delays.[22] To confirm that the MultiCP method is capable of quantitative ^{13}C analysis, acquisition parameters were calibrated and validated using model aromatic- and aliphatic-containing polymers PS and LDPE (Figure S6 in the supplementary information). Figure 7a shows the fitted peak of MultiCP ^{13}C NMR results of PVC residue. The NMR spectrum has two main groups of peaks, 20~ 60 ppm, and 120~150 ppm, which are assigned as the aliphatic and aromatic/alkene groups, respectively. There is another small signal observed at 15 ppm which is assigned as the primary carbon and can be regarded as an end group of the polymer. The peaks with asterisks indicate spinning side bands from the aromatic carbons, which are exactly 14 kHz on either side of the center band.

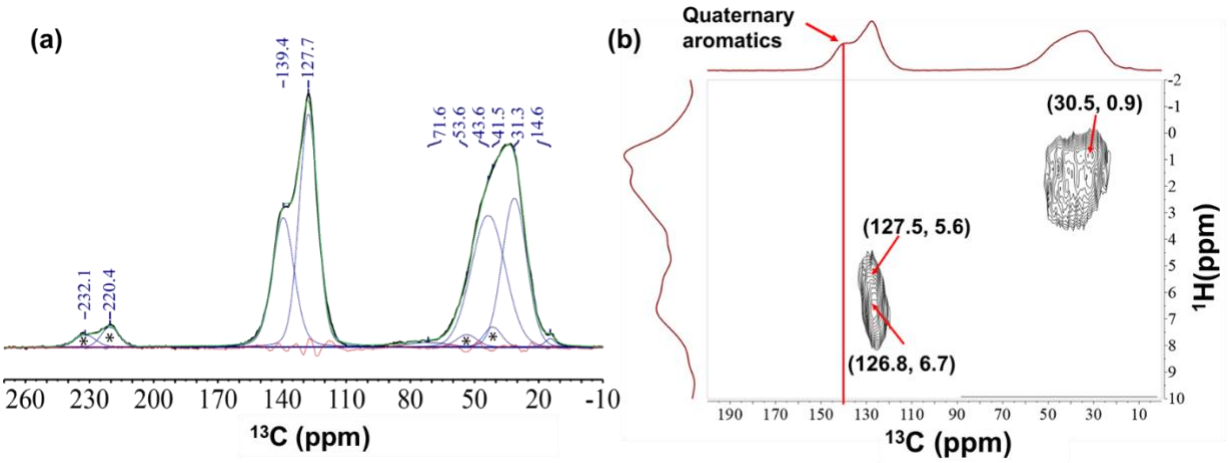

Figure 7. (a) Fitted peak results of MultiCP 13C solid-state NMR (b) 2D 13C-1H LG-HETCOR extracts 1H chemical shifts of PVC residue. The NMR data are shown in black, and each peak is labeled in blue, the fitted peak is shown in green, and the residue is shown in red.

To further support the assignments, we collected a 2D ^{13}C-^{1}H FSLG-HETCOR NMR experiment on the PVC residue, shown as Figure 7b. The signal near 137 ppm was confirmed quaternary, as they have no immediate protons, while the protonated C=C region near 127 ppm seems to have associations with two proton types, at roughly 6.6 and 5.5 ppm. The two proton types could refer to the hydrogen attached on a single C=C bond or π-conjugated C=C bonds but it is difficult to quantify the total amount of each type due to the resolution of the spectrum. We therefore must quantify the aromatic and alkene protonated C=C environments together. The quantification of different carbon species based on spectral deconvolution of MultiCP ^{13}C spectrum is shown in Table 4.

Table 4. Integrals of specific peaks corresponding to different carbon types obtained from ^{13}C MultiCP NMR analysis of PVC residue.

Carbon Type	Percent Area
Protonated C=C	33.2%
Quaternary Aromatics	22.6%
Aliphatic	42.5%
Primary C	0.8%
Unknowns	1.1%

4. Discussion

4.1 Kinetic model

PVC model II can predict the PVC decomposition accurately within a temperature range from 300 to 480 °C. Some error between the model and the experimental results occurs at the beginning of the dehydrochlorination (240-300 °C) and the end of the crosslinked intermediates decomposition stage (480-520 °C). At the lower temperature range, from 240 to 300 °C dehydrochlorination likely starts at PVC structure defect sites that are thermally labile without autocatalysis.[25] When the quantities of HCl and polyenes reach a specific point, they react to generate polyenyl cation radicals, which promote autocatalysis.[22, 25] While the model we built is a lumped model fitted by nonlinear least error regression, the model fits well to the kinetics that represent the entire dehydrochlorination process. The empirical fitted activation energy value is lower than the non-catalyzed dehydrochlorination values reported by DFT,[47] but

is in reasonable agreement with the computed activation energies for HCl catalyzed dehydrochlorination of chlorinated segments adjacent to alternating single and double C–C bonds. Figure 6a demonstrates that our model can predict the PVC degradation under autocatalytic conditions and shows the model can predict the residual Cl when the residual Cl level is higher than 0.1 wt.%. However, when the level of residual Cl is less than 0.1 wt.%, the autocatalytic effect does not occur due to the low Cl concentration. Therefore, our model is not sensitive enough to predict the residual Cl for 8h pretreatments which has a 0.03 wt.% of the Cl content.

4.2 Structure of PVC residue

The high concentration of the quaternary aromatic carbons (Table 4) indicates high concentration of crosslinked intermediates. Starnes reported the most likely crosslinked intermediate center in dehydrochlorinated PVC is cyclohexene that forms by intermolecular reactions with two polyene chains.[22] The maximum quaternary carbons would be two if cyclohexene is the crosslinked center (Figure 8a). However, if the cyclohexene is the most abundant structure, all aliphatic carbons must contribute to the crosslinked center and all HC=C bonds would form the surrounding structure. A surrounding chain with all HC=C bonds is not stable at high temperatures,[62] hence cyclohexene is less likely to be the most abundant structure of crosslinked centers in pretreated PVC.

We propose that cyclohexadiene is a more probable crosslinked center structure based on the carbon balance calculated from Table 4 as shown in Figure 8b and 8c. The formation of cyclohexadiene has two possible explanations. First, the cyclohexene center is formed but is not stable. Thus, hydrogen transfers from the crosslinked centers to the surrounding structures at 320 °C, resulting in the formation of cyclohexadiene center. Second, the formation of crosslinked intermediates could be more complex than the mechanism proposed in the literature,[22] as more than two polyene chains can react with each other and form a crosslinked center.

The high percentage of quaternary carbon indicates a high concentration of crosslinked centers. If the cyclohexadiene obtains three quaternary carbons, the crosslink concentration in the PVC residue will be approximately 50% and the surrounding chain would be composed of C=C and aliphatic groups with a 1:1 ratio. If the cyclohexadiene has two quaternary carbons, the crosslink concentration would be around 67%, and the surrounding chain will be composed of C=C and aliphatic groups with a 1 to 2 ratio. A small amount of char precursor (Figure 8d) could be formed at 320 °C with aromatics as the center structure, which would reduce the amount of the quaternary carbon contributing to the crosslinked center.

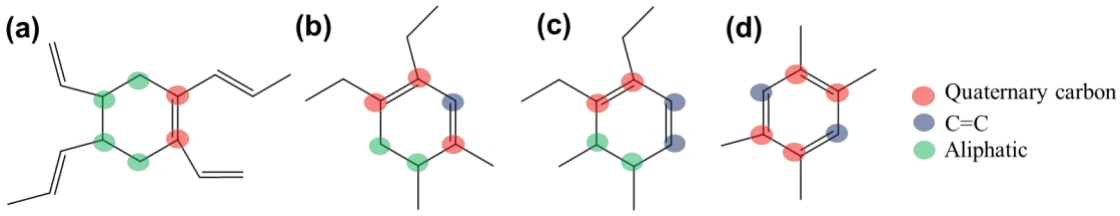

Figure 8. Proposed crosslinked center structure with (a) cyclohexene, (b) cyclohexadiene with three quaternary carbons, (c) cyclohexadiene with two quaternary carbons, (d) benzene with four quaternary carbons as a char precursor.

4.3 PVC decomposition reaction pathway

A reaction pathway for the decomposition of PVC is shown in Figure 9. The first step in this process is the dehydrochlorination to form HCl and linear polyenes with a rate constant of k_1. The

dehydrochlorination is catalyzed by HCl, which also appears to catalyze the formation of benzene (see Figure 3 and Figure 5).[47] As HCl is eliminated, the generated polyenes have a π-conjugated structure and start to cyclize to form crosslinked segments through intermolecular reactions.[29] The crosslinked intermediates are likely to be composed of cyclohexadiene as the crosslinked center structure and LDPE-like structures with random double bonds in the surrounding chains. The structure of the crosslinked intermediates is discussed in Section 4.2. As the temperature increases, the crosslinked intermediates continue to decompose and generate aromatic and polyaromatics, as well as non-condensable products (k_3). The formation of aromatics and non-condensable gas from the crosslinked intermediates can be considered parallel first order reactions. The intermediates will further convert into polyaromatics, or chars (written as 2C in Figure 9) after all volatile components are removed.

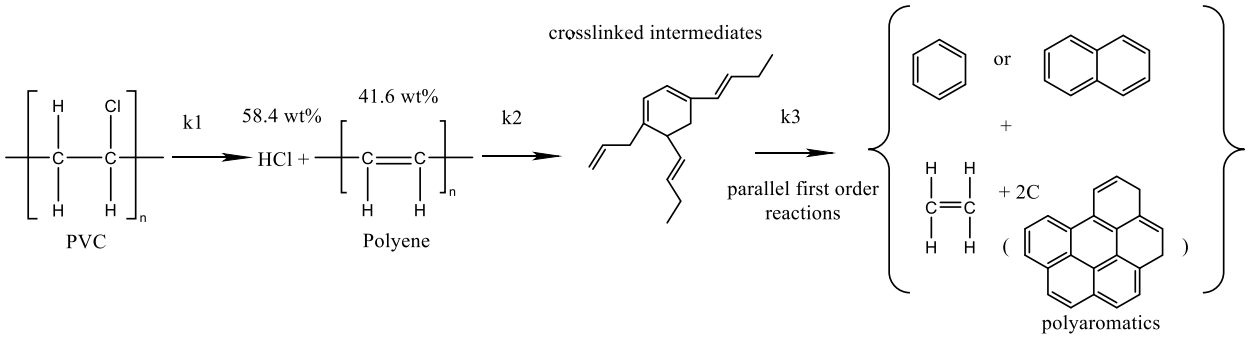

Figure 9. Proposed reaction pathway for PVC thermal decomposition.

5. Conclusions

PVC decomposes at temperatures between 250 and 320 °C to form HCl, small amounts of benzene, and a solid residue of crosslinked backbones containing LDPE-like polyene as the surrounding chain with cyclohexadiene as the most probable crosslinked center. Up to 99.7% percent of Cl is removed during inert thermal treatment of PVC at 320 °C after 20 min. The formation rates of HCl and benzene have a similar trend which indicates that formation of benzene is likely catalyzed by HCl in the first stage of thermal decomposition, a finding corroborated by both TGA results and DFT calculations. The crosslinked intermediates contain 22.6% of quaternary carbons which indicates a high crosslink concentration. In other words, 50-67% of the carbon in the solid residue contributes to forming crosslinked centers. The solid residue continues to decompose in the range of 320-600 °C along with the production of small amounts of non-condensable gases and large amounts of aromatics. The crosslinked polymer backbone does not decompose and instead forms carbon-rich polyaromatic chars. The overall PVC decomposition could be regarded as the combination of a first order dehydrochlorination reaction and a parallel first order crosslinked intermediates decomposition. The dehydrochlorination reaction is likely an autocatalytic reaction catalyzed by HCl. The apparent activation energy that fits our experimental data for dehydrochlorination is 116 kJ/mol (according to TGA), which is in reasonable agreement with the DFT prediction of 135 kJ/mol. The apparent activation energy for the crosslinked intermediates decomposition is estimated at 231 kJ/mol.

The model in this paper predicts Cl removal during PVC thermal pretreatment accurately. The model can help design Cl removal pretreatment before pyrolyzing post-waste plastic that contains PVC. FT-IR and Solid-state 2D NMR was used to study the structure of the dehydrochlorinated PVC. These results provide more information on the intermediate product structures formed during PVC pyrolysis, and insights on PVC pyrolysis chemistry.

6. Acknowledgements

This material was based upon work supported by the U.S. Department of Energy, Office of Energy Efficiency and Renewable Energy, Bioenergy Technologies Office under Award Number DEEE0009285. This work was also partially authored in part by the National Renewable Energy Laboratory, operated by Alliance for Sustainable Energy, LLC, for the U.S. Department of Energy (DOE) under contract no. DE-AC36-08GO28308. Funding was provided by the US Department of Energy Office of Energy Efficiency and Renewable Energy Bioenergy Technologies Office. We used resources at the National Energy Research Scientific Computing Center, a DOE Office of Science User Facility that is supported by the DOE, Office of Science, under contract no. DE-AC02-05CH11231 using NERSC award BES-ERCAP0027367. Part of the computational work was carried out using supercomputing resources at the Center for Nanoscale Materials (CNM), a DOE Office of Science User Facility located at Argonne National Laboratory that is supported by DOE contract DE-AC02-06CH11357. The views expressed in the article do not necessarily represent the views of the DOE or the U.S. Government. The U.S. Government retains and the publisher, by accepting the article for publication, acknowledges that the U.S. Government retains a nonexclusive, paid-up, irrevocable, worldwide license to publish or reproduce the published form of this work, or allow others to do so, for U.S. Government purposes.

References

1. Nicholson, S. R.; Rorrer, N. A.; Carpenter, A. C.; Beckham, G. T., Manufacturing energy and greenhouse gas emissions associated with plastics consumption. *Joule* **2021,** *5* (3), 673-686.
2. *Chemical Economics Handbook: Polyvinyl Chloride Resins - CEH*; 2020.
3. Goswami, T. K.; Mangaraj, S., 8 - Advances in polymeric materials for modified atmosphere packaging (MAP). In *Multifunctional and Nanoreinforced Polymers for Food Packaging*, Lagarón, J.-M., Ed. Woodhead Publishing: 2011; pp 163-242.
4. Emblem, A., 13 - Plastics properties for packaging materials. In *Packaging Technology*, Emblem, A.; Emblem, H., Eds. Woodhead Publishing: 2012; pp 287-309.
5. PVC in PET Bottle Recycling. https://www.petbottlewashingline.com/pvc-in-pet-bottle-recycling/.
6. Miandad, R.; Barakat, M. A.; Aburiazaiza, A. S.; Rehan, M.; Ismail, I. M. I.; Nizami, A. S., Effect of plastic waste types on pyrolysis liquid oil. *International Biodeterioration & Biodegradation* **2017,** *119*, 239-252.
7. Paci, M.; La Mantia, F. P., Influence of small amounts of polyvinylchloride on the recycling of polyethyleneterephthalate. *Polymer Degradation and Stability* **1999,** *63* (1), 11-14.
8. Ma, J.; Tominac, P. A.; Aguirre-Villegas, H. A.; Olafasakin, O. O.; Wright, M. M.; Benson, C. H.; Huber, G. W.; Zavala, V. M., Economic evaluation of infrastructures for thermochemical upcycling of post-consumer plastic waste. *Green Chemistry* **2023,** *25* (3), 1032-1044.
9. Barbaroux, M.; Horowski, B.; Mokuolu, S.; Petrich, M. A.; Snyder, M.; Whitford, W. G.; Committee, B. S. The Green Imperative: Part Two — Engineering for Sustainability in Single-Use Technologies. https://bioprocessintl.com/manufacturing/single-use/the-green-imperative-part-two-engineering-for-the-new-plastics-economy-and-sustainability-in-single-use-technologies/.
10. Kusenberg, M.; Zayoud, A.; Roosen, M.; Thi, H. D.; Abbas-Abadi, M. S.; Eschenbacher, A.; Kresovic, U.; De Meester, S.; Van Geem, K. M., A comprehensive experimental investigation of plastic waste pyrolysis oil quality and its dependence on the plastic waste composition. *Fuel Processing Technology* **2022,** *227*, 107090.
11. Li, H.; Aguirre-Villegas, H. A.; Allen, R. D.; Bai, X.; Benson, C. H.; Beckham, G. T.; Bradshaw, S. L.; Brown, J. L.; Brown, R. C.; Castillo, M. A. S., Expanding Plastics Recycling Technologies: Chemical Aspects, Technology Status and Challenges. **2022**.
12. Kusenberg, M.; Eschenbacher, A.; Djokic, M. R.; Zayoud, A.; Ragaert, K.; De Meester, S.; Van Geem, K. M., Opportunities and challenges for the application of post-consumer plastic waste

pyrolysis oils as steam cracker feedstocks: To decontaminate or not to decontaminate? *Waste Management* **2022,** *138*, 83-115.
13. Okuwaki, A., Feedstock recycling of plastics in Japan. *Polymer Degradation and Stability* **2004,** *85* (3), 981-988.
14. Fukushima, M.; Wu, B.; Ibe, H.; Wakai, K.; Sugiyama, E.; Abe, H.; Kitagawa, K.; Tsuruga, S.; Shimura, K.; Ono, E., Study on dechlorination technology for municipal waste plastics containing polyvinyl chloride and polyethylene terephthalate. *Journal of Material Cycles and Waste Management* **2010,** *12* (2), 108-122.
15. Huang, J.; Li, X.; Zeng, G.; Cheng, X.; Tong, H.; Wang, D., Thermal Decomposition Mechanisms of Poly(Vinyl Chloride): A Computational Study. *Waste Management* **2018,** *76*, 483-496.
16. Lingaiah, N.; Uddin, M. A.; Muto, A.; Imai, T.; Sakata, Y., Removal of organic chlorine compounds by catalytic dehydrochlorination for the refinement of municipal waste plastic derived oil. *Fuel* **2001,** *80* (13), 1901-1905.
17. Scheirs, J.; Kaminsky, W., *Feedstock Recycling and Pyrolysis of Waste Plastics: Converting Waste Plastics into Diesel and Other Fuels*. John Wiley & Sons, Ltd: 2006.
18. Buekens, A.; Schoeters, J. *European experience in the pyrolysis and gasification of solid wastes*; American Institute of Chemical Engineers, New York, NY: 1985.
19. Nagu, M.; Alanazi, N.; Adam, F., Organochloride Contamination in a Refinery Naphtha Hydrotreater Unit. *Materials performance* **2017,** *56*.
20. SELECTION OF STAINLESS STEELS FOR HANDLING HYDROCHLORIC ACID (HCL). https://bssa.org.uk/bssa_articles/9-selection-of-stainless-steels-for-handling-hydrochloric-acid-hcl/ (accessed 11/12).
21. Hjertberg, T.; Sörvik, E. M., Formation of anomalous structures in PVC and their influence on the thermal stability: 3. Internal chloroallylic groups. *Polymer* **1983,** *24* (6), 685-692.
22. Starnes, W. H., Structural and mechanistic aspects of the thermal degradation ofpoly(vinyl chloride). *Progress in Polymer Science* **2002,** *27*.
23. LópezI, A.; Marco, I. d.; Laresgoiti, B. M. C. M. F.; Adrados, A., Dechlorination of fuels in pyrolysis of PVC containing plastic wastes. *Fuel Processing Technology* **2011,** *92* (2), 253-260.
24. Jordan, K. J.; Suib, S. L.; Koberstein, J. T., Determination of the Degradation Mechanism from the Kinetic Parameters of sDehydrochlorinated Poly(vinyl chloride) Decomposition. *The Journal of Physical Chemistry B* **2001,** *105*, 3174-3181.
25. Starnes, W. H.; Ge, X., Mechanism of Autocatalysis in the Thermal Dehydrochlorination of Poly(vinyl chloride). *Macromolecules* **2004,** *37*, 352-359.
26. B.B.TroitskiiL, S.Troitskaya, A.S.Yakhnov, M.A.Novikova, V.N.Denisova, V.K.Cherkasov, M.P.Bubnov, Investigation of autocatalytic thermal degradation of poly(vinyl chloride) by ESR spectroscopy. *Polymer Degradation and Stability* **1997,** *58*, 83-89.
27. Starnes, W. H., Overview and assessment of recent research on the structural defects in poly(vinyl chloride). *Polymer Degradation and Stability* **2012,** *97* (9), 1815-1821.
28. Xie, T. Y.; Hamielec, A. E.; Rogestedt, M.; Hjertberg, T., Experimental investigation of vinyl chloride polymerization at high conversion: polymer microstructure and thermal stability and their relationship to polymerization conditions *Polymer* **1994,** *35* (7).
29. McNeill, L. C.; Menetea, L.; Cole, W. J., A study of the products of PVC thermal degradation. *Polymer Degradation and Stability* **1995,** *49* (1), 181-191.
30. Marongiu, A.; Faravelli, T.; Bozzano, G.; Dente, M.; Ranzi, E., Thermal degradation of poly(vinyl chloride). *Journal of Analytical and Applied Pyrolysis* **2003**.
31. KnÜMann, R.; Bockhorn, H., Investigation of the Kinetics of Pyrolysis of PVC by TG-MS-Analysis. *Combustion Science and Technology* **1994,** *101* (1-6), 285-299.
32. Beltrán, M.; Marcilla, A., Thermogravimetric kinetic study of poly(vinyl chloride) pyrolysis. *Polymer Degradation and Stability* **1995**.

33. Xu, Z.; Kolapkar, S. S.; S, Z.; Bar-Ziv, E.; McDonald, A. G., Comprehensive kinetic study of thermal degradation of polyvinylchloride (PVC). *Polymer Degradation and Stability* **2020,** *176*, 109148.
34. Gui, B.; Qiao, Y.; Wan, D.; Liu, S.; Han, Z.; Yao, H.; Xu, M., Nascent tar formation during polyvinylchloride (PVC) pyrolysis. *Proceedings of the Combustion Institute* **2013,** *34* (2), 2321-2329.
35. Purmova, J.; Pauwels, K. F. D.; Zoelen, W. v.; Vorenkamp, E. J.; Schouten, A. J., New Insight into the Formation of Structural Defects in Poly(Vinyl Chloride). *Macromolecules* **2005,** *38*, 6352-6366.
36. Kim, S., Pyrolysis kinetics of waste PVC pipe. *Waste Management* **2001,** *21* (7), 609-616.
37. Petre, A. L.; Budrugeac, P.; segal, E., Thermal Degradation of Polyvinyl Chloride. *Journal of Thermal Analysis and Calorimetry* **1999,** *56*, 1065-1070.
38. Wu, C.-H.; Chang, C.-Y.; Hor, J.-L.; Shih, S.-M.; Chen, L.-W.; Chang, F.-W., Two-Stage pyrolysis model of PVC. **1994,** *72* (4), 644-650.
39. Rehmann, L.; Prpich, G. P.; Daugulis, A. J., Remediation of PAH contaminated soils: Application of a solid–liquid two-phase partitioning bioreactor. *Chemosphere* **2008,** *73* (5), 798-804.
40. Duan, P.; Schmidt-Roh, K., Composite-pulse and partially dipolar dephased multiCP for improved quantitative solid-state 13C NMR. *Journal of Magnetic Resonance* **2017,** *285*, 68-78.
41. B.-J. van Rossum, H. F., H.J.M.de Groota, High-Field and High-Speed CP-MAS13C NMR Heteronuclear Dipolar-Correlation Spectroscopy of Solids with Frequency-Switched Lee–Goldburg Homonuclear Decoupling. *Journal of Magnetic Resonance* **1996,** *124* (2), 516-519.
42. Stievano, L.; Tielens, F.; Lopes, I.; Folliet, N.; Gervais, C.; Costa, D.; Lambert, J.-F., Density Functional Theory Modeling and Calculation of NMR Parameters: An ab Initio Study of the Polymorphs of Bulk Glycine. *Crystal Growth & Design* **2010,** *10*, 3657-3667.
43. Paruzzo, F. M.; Emsley, L., High-resolution 1H NMR of powdered solids by homonuclear dipolar decoupling. *Journal of Magnetic Resonance* **2019,** *309*.
44. Robb, M. A. C., J. R.; Scalmani, G.; Barone, V.; Mennucci, B.; Petersson, G. A.; Nakatsuji, H.; Caricato, M.; Li, X.; Hratchian, H. P.; Izmaylov, A. F.; Bloino, J.; Zheng, G.; Sonnenberg, J. L.; Hada, M.; Ehara, M.; Toyota, K.; Fukuda, R.; Hasegawa, J.; Ishida, M.; Nakajima, T.; Honda, Y.; Kitao, O.; Nakai, H.; Vreven, T.; Jr., J. A. M.; Peralta, J. E.; Ogliaro, F.; Bearpark, M.; Heyd, J. J.; Brothers, E.; Kudin, K. N.; Staroverov, V. N.; Keith, T.; Kobayashi, R.; Normand, J.; Raghavachari, K.; Rendell, A.; Burant, J. C.; Iyengar, S. S.; Tomasi, J.; Cossi, M.; Rega, N.; Millam, J. M.; Klene, M.; Knox, J. E.; Cross, J. B.; Bakken, V.; Adamo, C.; Jaramillo, J.; Gomperts, R.; Stratmann, R. E.; Yazyev, O.; Austin, A. J.; Cammi, R.; Pomelli, C.; Ochterski, J. W.; Martin, R. L.; Morokuma, K.; Zakrzewski, V. G.; Voth, G. A.; Salvador, P.; Dannenberg, J. J.; Dapprich, S.; Daniels, A. D.; Farkas, O.; Foresman, J. B.; Ortiz, J. V.; Cioslowski, J.; Fox, D. J. *Gaussian 09*, Wallingford CT, 2013.
45. Zhao, Y.; Truhlar, D. G., Density Functionals with Broad Applicability in Chemistry. *Accounts of Chemical Research* **2008,** *41* (2), 157-167.
46. Zhao, Y.; Truhlar, D. G., The M06 Suite of Density Functionals for Main Group Thermochemistry, Thermochemical Kinetics, Noncovalent Interactions, Excited States, and Transition Elements: Two New Functionals and Systematic Testing of Four M06-Class Functionals and 12 Other Function. . *Theoretical Chemistry Accounts* **2008,** *120*, 215-241.
47. Papanikolaou, K. G.; Wu, J.; Huber, G. W.; Mavrikakis, M. J. J. o. P. R., Mechanistic insights into the pyrolysis of poly (vinyl chloride). **2023,** *30* (2), 83.
48. Grimes, S. M.; Lateef, H.; Jafari, A. J.; Mehta, L., Studies of the effects of copper, copper(II) oxideand copper(II) chloride on the thermaldegradation of poly(vinyl chloride). *Polymer Degradation and Stability* **2006,** *91*, 3274e3280.
49. Hjertberg, T.; Sörvik, E. M., Thermal Degradation of PVC. In *Degradation and Stabilisation of PVC*, Owen, E. D., Ed. Springer Netherlands: Dordrecht, 1984; pp 21-79.
50. Zhao, D.; Wang, X.; Miller, J. B.; Huber, G. W., The Chemistry and Kinetics of Polyethylene Pyrolysis: A Process to Produce Fuels and Chemicals. *ChemSusChem* **2020,** *13*, 1764-1774.
51. SEEGER, M.; GRITTER, R. J., Thermal Decomposition and Volatilization of Poly(α-olefins). *Journal of Polymer Science* **1977,** *15*, 1393-1402.
52. Akaike, H., A new look at the statistical model identification. *IEEE* **1974,** *19* (6), 716-723.

53. Aho, K.; Derryberry, D.; Peterson, T., Model selection for ecologists: the worldviews of AIC and BIC. *Ecology* **2014,** *95* (3), 631-636.
54. Brems, A.; Baeyens, J.; Vandecasteele, C.; Dewil, R., Polymeric Cracking of Waste Polyethylene Terephthalate to Chemicals and Energy. *Journal of the Air & Waste Management Association* **2011,** *61* (7), 721-731.
55. Socrates, G., Infrared and Raman Characteristic Group Frequencies: Tables and Charts. John Wiley & Sons: 2004; p. 20.
56. I.Z. Rakhmatullina; Efimova, S. V.; Tyurina, V. A.; Al-Muntaserb, A. A.; Klimovitskiib, A. E.; Varfolomeevb, M. A.; Klochkov, V. V., Application of high resolution NMR (1H and 13C) and FTIR spectroscopy for characterization of light and heavy crude oils. *Journal of Petroleum Science and Engineering* **2018,** *168*, 256-262.
57. Barreiro, D. L.; S.Riede; U.Hornung; A.Kruse; Prins, W., Hydrothermal liquefaction of microalgae: Effect on the product yields of the addition of an organic solvent to separate the aqueous phase and the biocrude oil. *Algal Research* **2015,** *12*, 206-212.
58. Solà, M., Aromaticity rules. *Nature Chemistry* **2022,** *14*, 585-590.
59. Roucoules, V.; Fail, C. A.; Schofield, W. C. E.; Teare, O. H.; Badyal, J. P. S., Diels-Alder Chemistry on Alkene Functionalized Films. *Langmuir* **2005,** *21*, 1412-1415.
60. Smith, B. C., Group Wavenumbers and an Introduction to the Spectroscopy of Benzene Rings. *Spectroscopy* **2016,** *31*, 34-37.
61. Zou, S.; Wu, Y.; Yang, M.; Lic, C.; Tong, J., Bio-oil production from sub- and supercritical water liquefaction of microalgae Dunaliella tertiolecta and related properties. *Energy & Environmental Science* **2010,** *3*.
62. Kohler, B. E.; Spangler, C.; Westerfield, C., The 2 1Ag state in the linear polyene 2,4,6,8,10,12,14,16-octadecaoctaene. *The Journal of Chemical Physics* **1988,** *89* (9), 5422-5428.